

**SDS observation in  
East Asia**

Y. Q. Wang et al.

# Surface observation of sand and dust storm in East Asia and its application in CUACE/Dust

Y. Q. Wang<sup>1</sup>, X. Y. Zhang<sup>1</sup>, S. L. Gong<sup>1,2</sup>, C. H. Zhou<sup>1</sup>, X. Q. Hu<sup>3</sup>, H. L. Liu<sup>1</sup>,  
T. Niu<sup>1</sup>, and Y. Q. Yang<sup>1</sup>

<sup>1</sup>Laboratory of Atmospheric Chemistry, Centre for Atmosphere Watch and Services, Chinese Academy of Meteorological Sciences, Beijing, China

<sup>2</sup>Air Quality Research Division, Science and Technology Branch, Environment Canada, Toronto, Canada

<sup>3</sup>National Meteorological Satellite Center, CMA, Beijing, China

Received: 19 March 2007 – Accepted: 15 June 2007 – Published: 27 June 2007

Correspondence to: Y. Q. Wang (wangyq@cams.cma.gov.cn)

Title Page

Abstract

Introduction

Conclusions

References

Tables

Figures

◀

▶

◀

▶

Back

Close

Full Screen / Esc

Printer-friendly Version

Interactive Discussion

EGU

## Abstract

The spatial-temporal distributions and sources of sand and dust storm (SDS) in East Asia from 2001 to 2006 were investigated on the basis of visibility and PM<sub>10</sub> data from the routine SDS and weather monitoring networks run by CMA (China Meteorological Administration). A power functional relationships between PM<sub>10</sub> and visibility was found among various regions generally with a good correlation ( $r^2=0.90$ ), especially in Asian SDS source regions. In addition, three SDS occurrence centers, i.e. western China, Mongolia and northern China, were identified with the Mongolia source contributing more dust to the downwind areas including Korea and Japan than other two sources. Generally, high PM<sub>10</sub> concentrations were observed in most areas of northern China. The highest value was obtained in the center of western China with a spring daily mean value of  $876 \mu\text{g m}^{-3}$ , and the value in other source regions exceeds  $200 \mu\text{g m}^{-3}$ . These data sets together with the satellite observations in China form the main observation database for the evaluation and data assimilation of CUACE/Dust system – an operational SDS forecasting system for East Asia.

## 1 Introduction

In each spring, the Asian SDS originating from the arid and semi-arid regions of China and Mongolia greatly increases the particulate concentrations locally, regionally and even globally in some events, resulting in significant visibility reduction, respiratory symptoms, eye trouble to human beings as well as damages to animals, plants, industry and social activities (Kim et al., 2001; Seinfeld et al., 2004; Zhang et al., 1993). As one type of severe disaster weather, SDS was highly concerned by the government and people in China and downwind countries in each spring.

As a natural phenomenon, SDS has been recorded from the Diary of Tonghe Weng, which indicated that the average of annual dusty days in Beijing was over nine during 1860–1898 AD (Fei et al., 2005). However, a systematical monitoring of SDS events

## SDS observation in East Asia

Y. Q. Wang et al.

Title Page

Abstract

Introduction

Conclusions

References

Tables

Figures

◀

▶

◀

▶

Back

Close

Full Screen / Esc

Printer-friendly Version

Interactive Discussion

**SDS observation in  
East Asia**

Y. Q. Wang et al.

Title Page

Abstract

Introduction

Conclusions

References

Tables

Figures

◀

▶

◀

▶

Back

Close

Full Screen / Esc

Printer-friendly Version

Interactive Discussion

was established in China only about half a century ago. As part of the routine weather monitoring network (Fig. 1), the visual visibility was recorded in China from 1950's as a mean to monitor the SDS events. The sources, spatial and temporal variation, dust deposition and regional characteristics of SDS have been studied using the dataset (Qian et al., 2004; Sun et al., 2001; Wang et al., 2005; Zhou, 2001; Zhou and Zhang, 2003). A similar dataset was also used to investigate the SDS characteristics in Mongolia (Natsagdorj et al., 2003). But the above studies did not cover the data in recent years when significant spatial and temporal variations of SDS were observed. Furthermore, these data are primarily qualitative as only the SDS category was reported. To obtain the dust particle concentrations during SDS events, CMA established a SDS monitoring network with 19 stations located in SDS source and downwind regions in northern China with PM<sub>10</sub> (particles with diameter less than 10 μm) observations (Fig. 1) since 2003. Eleven of them are also equipped with the instrumental visibility measurements.

These two networks provide near real-time distributions of SDS in China for characterizing SDS and model validation. This paper presents the meteorological recorded SDS data in spring from 2001 to 2006, PM<sub>10</sub> and visibility data at the SDS observation stations in spring from 2004 to 2006. The specific objectives of the studies reported here were to (1) characterize the spatial distribution and temporal variation of the frequency of SDS events in recent years; (2) investigate the PM<sub>10</sub> characteristics of northern China in SDS season; (3) find the relationship between PM<sub>10</sub> and visibility especially in SDS events; (4) introduce the model verification result based on this dataset.

Finally, these observational data together with satellite observations (Hu et al., 2007) will facilitate the evaluation and data assimilation of the CMA operational SDS forecasting model – CUACE/Dust (Chinese Unified Atmospheric Chemistry Environment – Dust) (Gong and Zhang, 2007<sup>1</sup>; Zhou et al., 2007) for the model improvements and

<sup>1</sup>Gong, S. L. and Zhang, X. Y.: CUACE/Dust – An integrated system of observation and modeling systems for operational dust forecasting system in Asia, Atmos. Chem. Phys. Discuss., submitted, 2007.

initial forecasting conditions (Niu et al., 2007).

## 2 SDS observation data

### 2.1 Meteorological records related to SDS weather

Fig. 1 shows the distribution of the weather stations in China and surrounding countries. Most stations were located in east and south areas of China with high economy development, but in the Gobi desert and sandy land areas, the sources of SDS, the distribution of the weather stations is very sparse. In the meteorological records of China, four categories of SDS events including suspended dust (horizontal visibility less than 10 000 m, and very low wind speed), blowing dust (visibility reduce to 1000–10 000 m), sand and dust storm (visibility less than 1000 m) and severe sand and dust storm (visibility less than 500 m) are usually reported in the daily observation. The last three categories of dust events all result from strong winds. Through a data transfer system in CMA, the near real-time SDS observation data with 3-h interval at these stations were obtained. The SDS weather data in spring from 2001 to 2006 were used in this study.

### 2.2 PM<sub>10</sub> and visibility data

The 19 SDS stations with PM<sub>10</sub> observation are located in SDS source and down-wind regions in northern China (Fig. 1). A Tapered Element Oscillating Microbalance (TEOM, model 1400a, Rupprecht and Patashnick) operated at a controlled flow rate of 4 L/min was used to record continuously the PM<sub>10</sub> mass concentrations averaged over 5 min periods in each station. At eleven of the stations 5-min visibilities were also observed automatically on-line using FD-12 (Vaisala). From 2004, the PM<sub>10</sub> and visibility observation data were started to be transferred to the CMA information center in real-time. Detailed station information are described in Table 1.

Title Page

Abstract

Introduction

Conclusions

References

Tables

Figures

◀

▶

◀

▶

Back

Close

Full Screen / Esc

Printer-friendly Version

Interactive Discussion

### 3 Sand and dust storm occurrences in East Asia

#### 3.1 Spatial distribution and sources

The days of SDS events distinguished from the meteorological records of each weather station in every spring were calculated. Figure 2 shows the distribution of annual mean days of SDS events for all four categories SDS in spring from 2001 to 2006. There are three SDS centers in East Asia. One is the western China source including the Taklimakan Desert and surrounding area; the other is Mongolia source including the desert and semi-desert area in south of Mongolia; and the last one locates in northern China source region including the Badain Jaran Desert, the Tengger Desert, the Ulan Buh Desert and the Onqin Daga sandy land. Comparing with Mongolia source, northern China source has much less SDS events occurred in spring from 2001 to 2006. The three centers were also identified as the major Asian dust aerosol sources with about 70% dust emission through simulation study over past 43 years (Zhang et al., 2003). Another SDS center is located in northern India and Afghanistan, but it is not the SDS source to East Asia and will not be discussed further in this paper. The figure shows SDS events were also observed in Korea, Japan and south of China around Yangzi River.

The spatial distribution of each SDS type was shown in Fig. 3. Suspended dust event, also called dust fall event, often occurred in the downwind direction of SDS with large amount of dust deposition and very low wind speed. The highest frequency of suspended dust events occurred in the western China source (Fig. 3a), indicating that most of dust emitted from the Taklimakan Desert deposited in the desert again. The dust depositions also occurred in large downwind areas including east and south of China, Korea and Japan. This result is similar to the dust deposition flux estimation (Zhang et al., 1998) and the study using the data during 1960–1999 (Sun et al., 2001), but no high frequent suspended dust event was observed in the Loess Plateau. Both Mongolia source and the northern China source are centers of blowing sand events which also influenced whole Mongolia and most area of north China (Fig. 3b). In all of

## SDS observation in East Asia

Y. Q. Wang et al.

Title Page

Abstract

Introduction

Conclusions

References

Tables

Figures

◀

▶

◀

▶

Back

Close

Full Screen / Esc

Printer-friendly Version

Interactive Discussion

the three SDS sources, SDS and severe SDS events were observed, but high frequent events occurred in the Mongolia source (Figs. 3c, d).

The dust deposition result indicates that although many SDS events occurred in the western China source, they do not contribute very much to the east downwind area including east of China, Korea and Japan recently. Most of dust particles associated with SDS influenced to these areas were mainly from the Mongolia source and the northern China source during recent years. It is consistent with our previous study using back-trajectory combined PM<sub>10</sub> analysis (Wang et al., 2006, 2004) and the study by Sun et al. (2001). The spatial distribution of SDS event days indicates that the Mongolia source is more important than the northern China source in these years due to more SDS events observed. Zhang et al. (1997) reported that most of dust are transported northerly during relative warm and humid climate condition, like interglacial, and more dust delivered via northwesterly when dry and cold climate occurred during glacial. Based on experimental simulation results, Gong et al. (2004) found that the contributions of surface concentrations from non-Chinese deserts account for up to 60% in Northeast China and up to 50% in Korea and Japan.

### 3.2 Time series and variation

From the 1950's when the weather monitoring network of China started to operate, SDS frequency shows a generally descending trend since the early of 1960's in most areas of northern China except in the desertification regions such as the Onqin Daga sandy land (Zhang et al., 2003; Zhou, 2001; Zhou and Zhang, 2003). From 2000 and 2001, the frequency began to rise, reaching a relatively peak in 2001 then dropping again in 2002 (Zhang et al., 2003; Zhou and Zhang, 2003). Figure 4 shows the annual variance of SDS occurrence during the springtime 2001–2006. Higher SDS frequency and larger influencing areas were observed in 2001 and 2006 than the years of 2002, 2003, 2004 and 2005. In the western China source, the SDS occurrence is relatively stable during these years while the sharp variance could be seen in the Mongolia source and the northern China source. Compared with the observation in 1960–1999

## SDS observation in East Asia

Y. Q. Wang et al.

Title Page

Abstract

Introduction

Conclusions

References

Tables

Figures

◀

▶

◀

▶

Back

Close

Full Screen / Esc

Printer-friendly Version

Interactive Discussion

(Sun et al., 2001), the SDS center location is shift northerly to Mongolia, and the Loess Plateau is no longer a significant deposition region in recent years.

## 4 PM<sub>10</sub> and visibility characteristics

### 4.1 PM<sub>10</sub> concentration and visibility measurement results

5 The mean daily PM<sub>10</sub> concentrations and visibility were illustrated for each SDS station for all spring data during 2004 to 2006 in Fig. 5. The highest PM<sub>10</sub> concentrations with mean values of 876 and 703  $\mu\text{g m}^{-3}$  were observed at the stations of Tazhong and Hetian which are located in the center and southern margin of the Taklimakan Desert, the western China source for Asian SDS. This is consistent with the frequency of SDS  
10 events occurring in this region (Fig. 2). The highest daily averaged PM<sub>10</sub> concentration at Tazhong station is 7414  $\mu\text{g m}^{-3}$  and the 5-min data often exceeds the upper limit of the instrument of 10 000  $\mu\text{g m}^{-3}$ . At Zhurihe station in Onqin Daga sandy land, east part of SDS northern China source, PM<sub>10</sub> concentration is also high with the mean value of 335  $\mu\text{g m}^{-3}$ . Mean PM<sub>10</sub> concentration were observed to exceed 200  $\mu\text{g m}^{-3}$   
15 for Minqin, Dongsheng, Datong, Wulatezhongqi, Dunhuang, Ejinaqi and Yushe stations. At Beijing, a city in typical SDS transported area, mean PM<sub>10</sub> concentration is 180  $\mu\text{g m}^{-3}$ , and the highest concentration is 735  $\mu\text{g m}^{-3}$ . About half of the days in the spring seasons of the three years can be considered to be the polluted days by PM<sub>10</sub> concentration that is higher than the Class II Chinese daily PM<sub>10</sub> standard of 150  $\mu\text{g m}^{-3}$  (GB3095–1996).  
20

Due to the high frequency of SDS events, very low visibility was observed in Tazhong station with a mean value of 10 395 m. However, PM<sub>10</sub> concentration and visibility are not linearly correlated in the same manner over all regions in northern China, which is mainly because of different physical and chemical characteristics of the aerosol (Watson, 2002). Yushe is located in a coal enrichment area and infrequently impacted by  
25 SDS, its aerosol composition is quite different with Zhurihe located in a SDS source

Title Page

Abstract

Introduction

Conclusions

References

Tables

Figures

◀

▶

◀

▶

Back

Close

Full Screen / Esc

Printer-friendly Version

Interactive Discussion

region. This explains the fact that even though Yushe station has an mean daily  $\text{PM}_{10}$  concentration of  $200 \mu\text{g m}^{-3}$  that is lower than that at Zhurihe station, Yushe observes a lower visibility than Zhurihe.

Generally, SDS events are often associated with much higher mean  $\text{PM}_{10}$  concentrations and much lower mean visibility values than the entire period averages for all the stations (Fig. 5). At Tazhong station, the two values are  $2493 \mu\text{g m}^{-3}$  and 5926 m in SDS events. High  $\text{PM}_{10}$  concentrations were also observed in Dongsheng and Zhurihe stations with mean value of  $1705 \mu\text{g m}^{-3}$  and  $1588 \mu\text{g m}^{-3}$  respectively. More obvious increase in  $\text{PM}_{10}$  concentrations was observed in Dalian than Beijing during SDS events.

The annual variation of  $\text{PM}_{10}$  concentrations in spring exhibits different pattern in different area (Fig. 6a). In the western China source represented,  $\text{PM}_{10}$  concentrations ranked highest in spring of 2004 at their representative stations of Tazhong and Hetian, decreased dramatically in 2005, and then increased in spring of 2006. At the other stations near SDS northern China source regions,  $\text{PM}_{10}$  concentration reached the highest value in 2006. At the stations in downwind SDS area, the annual variation shows different pattern than the source region with relative higher  $\text{PM}_{10}$  concentration value in 2005. Most stations have the similar monthly variation of  $\text{PM}_{10}$  concentration with the highest value in April except Hetian and Hami with the highest value found in March. This is consistent with the high frequency of SDS occurrence in April in east Asia (Sun et al., 2001).

#### 4.2 The relationship between $\text{PM}_{10}$ concentration and visibility

The 5-min datasets from typical sites in major sources of Asian SDS were analyzed for hourly  $\text{PM}_{10}$  concentrations that compare with corresponding visibility data. The relationships between  $\text{PM}_{10}$  and visibility show good correlations ( $R^2$  larger than 0.60) by power function fitting for 3 spring data together at Tazhong, Zhurihe and Minqin, respectively (Fig. 7). At Zhangbei, a station located in downwind SDS area, the  $R^2$

Title Page

Abstract

Introduction

Conclusions

References

Tables

Figures

◀

▶

◀

▶

Back

Close

Full Screen / Esc

Printer-friendly Version

Interactive Discussion

**SDS observation in  
East Asia**

Y. Q. Wang et al.

Title Page

Abstract

Introduction

Conclusions

References

Tables

Figures

◀

▶

◀

▶

Back

Close

Full Screen / Esc

Printer-friendly Version

Interactive Discussion

decreases to 0.40, and the even lower  $R^2$  of 0.22 was found in Yushe station which was impacted by more anthropogenic aerosols, indicating that mineral aerosol has better power function relationship with visibility than the mixture of dust and anthropogenic aerosol. This is further illustrated by the same fitting for the data during SDS events only (Fig. 8). The  $R^2$  reaches about 0.90 at the three SDS stations in source regions, and increases to 0.67 in the downwind station of Zhangbei.

The main output of CUACE/Dust is the dust particle concentration, but visibility is used to distinguish the category of SDS traditionally. The general publics understand more easily about the categories of SDS rather than concentration amounts of dust. The three  $PM_{10}$  concentrations corresponding to the visibility of 500 m, 1000 m and 10 000 m were estimated by the fitting from the data set during SDS events (Table 2). The stations of Hami and Yushe were not presented in Table 2, because no enough parallel data were observed during SDS events. The best corresponding  $PM_{10}$  concentrations are found to be 14 889, 5572 and  $213 \mu\text{g m}^{-3}$ , respectively. Therefore, the tradition grads of the four categories of SDS weathers can be divided by hourly  $PM_{10}$  concentration ranges as follows:

- Suspended dust:  $200 \mu\text{g m}^{-3} \leq PM_{10}$  (with very low wind speed)
- Blowing dust:  $200 \mu\text{g m}^{-3} \leq PM_{10} < 5500 \mu\text{g m}^{-3}$
- Sand and dust storm:  $5500 \mu\text{g m}^{-3} \leq PM_{10} < 15\,000 \mu\text{g m}^{-3}$
- Severe sand and dust storm:  $15\,000 \mu\text{g m}^{-3} \leq PM_{10}$

## 5 Application of observation data in model verification

The ground-based observation data from the two networks and data from FY-2C satellite were assimilated in CUACE/Dust system to improve its initial SDS condition (Niu et al., 2007). They were also used to verify the SDS forecasting results from the modeled

concentration of DM40 (dust particle matter with diameter less than  $40\ \mu\text{m}$ ) (Zhou et al., 2007). The verification result shows the model captured the major SDS episodes in 2006 in terms of the particle concentrations and variations at most stations (Zhou et al., 2007). Compared to the weather monitoring network, the measurements made at the SDS stations is more quantitative but limited in spatial coverage (Fig. 1). For spatial verification of the model, the weather monitoring network is used. However, these weather stations represent only a few locations in SDS source regions where most SDS events occurred. This disadvantage could be partly overcome by using satellite data.

Grid to grid approach was used to do verification in our developed SDS verification system. The ground-based observation data were assigned to their located grids and the SDS data retrieval from FY-2C satellite were used to the grid without ground stations. A GIS (Geographical Information System) based verification system was developed in ArcView with Avenue language to compare the forecasting and observation data on each  $1^\circ \times 1^\circ$  grid.

The method for dichotomous forecast (Wilks, 1995) of SDS and non-SDS was used in this study. As the reference  $\text{PM}_{10}$  concentrations given above,  $200\ \mu\text{g m}^{-3}$  is the concentration threshold for SDS event from non-SDS event. Although the output of the model is DM40, this  $\text{PM}_{10}$  concentration could still be used because the main component of dust particles should be  $\text{PM}_{10}$  at this concentration especially with low wind speed. SDS category we used includes all categories of SDS weathers for meteorological observation. For the satellite observation, it implies that the IDDI index of SDS is higher or equal to 20 (Hu et al., 2007). Treat score (TS), false alarm ratio, miss ratio, accuracy and bias score were calculated from contingency table.

The spatial verification results show that in spring 2006 the daily-averaged TS values are 0.31, 0.23 and 0.21 for 24 h, 48 h and 72 h forecasting, respectively. During SDS events period TS value dramatically increased with the highest value of 0.63 for 24 h forecasting in 12 March when a big SDS event occurred. But in 1 March and 2 March, when no SDS event occurred, TS is 0.00. The SDS forecasts maintain high accuracy

**SDS observation in  
East Asia**

Y. Q. Wang et al.

Title Page

Abstract

Introduction

Conclusions

References

Tables

Figures

◀

▶

◀

▶

Back

Close

Full Screen / Esc

Printer-friendly Version

Interactive Discussion

with average value of 0.88. Verification in different regions indicates the model has better performance in Xinjiang province in western China with higher averaged TS value of 0.40. On each grid the comparison between forecast and observation of each day in spring was also carried on, so the temporal verification result of each grid was calculated. The result shows TS are high in the areas around deserts, Gobi deserts and sandy lands which are SDS sources. In most area the bias scores are around 1, but in north Xinjing area the model often has false alarm. In north of Tibetan and south of China are often missed by the forecasting system.

Another version of the model without data assimilation was also run in spring of 2006. The verification result shows that it has a less satisfactory performance on SDS forecast with TS of 0.22 for 24 h forecasting than the model with data assimilation. A detailed comparison of these results is presented in the paper of Niu et al. (2007).

## 6 Conclusions

The investigation based on the Asian SDS data from the meteorological stations from 2001 to 2006, PM<sub>10</sub> and visibility data from the SDS monitoring stations from 2004 to 2006 have found three high SDS occurrence areas located in western China, Mongolia and northern China. In the recent years, more SDS events occurred in 2001 and 2006, and most strong SDS events occurred in the Mongolia source. High PM<sub>10</sub> concentrations were always associated with high frequency of SDS events in most areas of northern China. The highest PM<sub>10</sub> concentrations were observed in the center of the western China source with mean daily value of 876  $\mu\text{g m}^{-3}$ . In east part of the northern China source this value is 335  $\mu\text{g m}^{-3}$ . Generally in downwind area, the mean daily PM<sub>10</sub> concentration exceeded 100  $\mu\text{g m}^{-3}$ . The annual variation of PM<sub>10</sub> concentration shows different patterns in different regions. The highest monthly mean daily PM<sub>10</sub> concentration was observed in April at most SDS stations.

Good correlations are found between PM<sub>10</sub> and visibility by power function fitting, especially during SDS condition at the source regions. Three reference PM<sub>10</sub> values

## SDS observation in East Asia

Y. Q. Wang et al.

Title Page

Abstract

Introduction

Conclusions

References

Tables

Figures

◀

▶

◀

▶

Back

Close

Full Screen / Esc

Printer-friendly Version

Interactive Discussion

of 200, 5500 and 15 000  $\mu\text{g m}^{-3}$  are estimated to classify the dust concentration from CUACE/Dust system to the categories of SDS weathers.

A SDS verification system was also developed based on ground-based observational data supplemented by the SDS data retrieval from FY-2C satellite. TS value of the SDS forecasting from CUACE/Dust system is 0.31 for 24 h forecasting. The model has a good performance in SDS forecasting in East Asia especially during large SDS events. The model without data assimilation has a lower TS of 0.22 for 24 forecasting.

*Acknowledgements.* This study was supported by grants from the National Basic Research Program of China (2006CB403701) and MOST (2004DIB3J115).

## References

- Fei, J., Zhou, J., Zhang, Q., and Chen, H.: Dust weather records in Beijing during 1860–1898 AD based on the Diary of Tonghe Weng, *Atmos. Environ.*, 39, 3943–3946, 2005.
- Gong, S. L., Zhang, X. Y., Zhao, T. L., and Barrie, L. A.: Sensitivity of Asian dust storm to natural and anthropogenic factors. *Geophys. Res. Lett.*, 31, L07210, doi:10.1029/2004GL019502, 2004.
- Hu, X. Q., Lu, N. M., Niu, T., and Zhang, P.: Operational retrieval of Asian sand and dust storm from FY-2C geostationary meteorological satellite and its Application to real time Forecast in Asia, *Atmos. Chem. Phys. Discuss.*, 7, 8395–8421, 2007, <http://www.atmos-chem-phys-discuss.net/7/8395/2007/>.
- Kim, K. W., Kim, Y. J., and Oh, S. J.: Visibility impairment during Yellow Sand periods in the urban atmosphere of Kwangju, Korea, *Atmos. Environ.*, 35, 5157–5167, 2001.
- Natsagdorj, L., Jugder, D., and Chung, Y. S.: Analysis of dust storms observed in Mongolia during 1937–1999, *Atmos. Environ.*, 37, 1401–1411, 2003.
- Niu, T., Gong, S. L., Zhu, G. F., Liu, H. L., Hu, X. Q., Zhou, C. H., and Wang, Y. Q.: Data assimilation of dust aerosol observations for CUACE/Dust forecasting system, *Atmos. Chem. Phys. Discuss.*, 7, 8309–8332, 2007, <http://www.atmos-chem-phys-discuss.net/7/8309/2007/>.
- Qian, W. H., Tang, X., and Quan, L. S.: Regional characteristics of dust storms in China, *Atmos. Environ.*, 38, 4895–4907, 2004.

Title Page

Abstract

Introduction

Conclusions

References

Tables

Figures

◀

▶

◀

▶

Back

Close

Full Screen / Esc

Printer-friendly Version

Interactive Discussion

**SDS observation in  
East Asia**

Y. Q. Wang et al.

[Title Page](#)[Abstract](#)[Introduction](#)[Conclusions](#)[References](#)[Tables](#)[Figures](#)[◀](#)[▶](#)[◀](#)[▶](#)[Back](#)[Close](#)[Full Screen / Esc](#)[Printer-friendly Version](#)[Interactive Discussion](#)

- Seinfeld, J. H., Carmichael, G. R., Arimoto, R., Conant, W. C., Brechtel, F. J., Bates, T. S., Cahill, T. A., Clarke, A. D., Doherty, S. J., Flatau, P. J., Huebert, B. J., Kim, J., Markowicz, K. M., Quinn, P. K., Russell, L. M., Russell, P. B., Shimizu, A., Shinozuka, Y., Song, C. H., Tang, Y. H., Uno, I., Vogelmann, A. M., Weber, R. J., Woo, J. H., and Zhang, X. Y.: ACE-ASIA – Regional climatic and atmospheric chemical effects of Asian dust and pollution, *B. Am. Meteorol. Soc.*, 85, 367–380, 2004.
- Sun, J., Zhang, M., and Liu, T.: Spatial and temporal characteristics of dust storms in China and its surrounding regions, 1960–1999: Relations to source area and climate, *J. Geophys. Res.*, 106, 10 325–10 333, 2001.
- Wang, S., Wang, J., Zhou, Z., and Shang, K.: Regional characteristics of three kinds of dust storm events in China, *Atmos. Environ.*, 39, 509–520, 2005.
- Wang, Y. Q., Zhang, X. Y., and Arimoto, R.: The Contribution from Distant Dust Sources to the Atmospheric Particulate Matter Loadings at XiAn, China during Spring, *Sci. Total Environ.*, 368, 875–883, 2006.
- Wang, Y. Q., Zhang, X. Y., Arimoto, R., Cao, J. J., and Shen, Z. X.: The transport pathways and sources of PM<sub>10</sub> pollution in Beijing during spring 2001, 2002 and 2003, *Geophys. Res. Lett.*, 31, L14110, doi:10.1029/2004GL019732, 2004.
- Watson, J.: Visibility: Science and Regulation, *J. Air Waste Manage.*, 52, 628–713, 2002.
- Wilks, D. S.: Statistical Methods in the Atmospheric Sciences, Academic Press, San Diego, 1995.
- Zhang, X. Y., Arimoto, R., and An, Z. S.: Dust emission from Chinese desert sources linked to variations in atmospheric circulation, *J. Geophys. Res.*, 102, 28 041–28 047, 1997.
- Zhang, X. Y., Arimoto, R., An, Z. S., Chen, T., Zhang, G. Y., Zhu, G. H., and Wang, X. F.: Atmospheric trace elements over source regions for Chinese dust: Concentrations, sources and atmospheric deposition on the Loess Plateau, *Atmos. Environ.*, 27, 2051–2067, 1993.
- Zhang, X. Y., Arimoto, R., Zhu, G. H., Chen, T., and Zhang, G. Y.: Concentration, size-distribution and deposition of mineral aerosol over Chinese desert regions, *Tellus*, 50B, 317–330, 1998.
- Zhang, X. Y., Gong, S. L., Zhao, T. L., Arimoto, R., Wang, Y. Q., and Zhou, Z. J.: Sources of Asian dust and role of climate change versus desertification in Asian dust emission, *Geophys. Res. Lett.*, 30, 2272, doi:10.1029/2003GL018206, 2003.
- Zhou, Z. J.: Blowing-sand and sandstorm in China in recent 45 years, *Quaternary Sciences*, 21, 9–17 (in Chinese), 2001.

Zhou, Z. J. and Zhang, G. C.: Typical severe dust storms in northern China during 1954–2002, Chinese Sci. Bull., 48, 2366–2370, 2003.

Zhou, C. H., Gong, S. L., Zhang, X. Y., Wang, Y. Q., Niu, T., Liu, H. L., Zhao, T. L., Yang, Y. Q., and Hou, Q.: Development and evaluation of an operational SDS forecasting system for

5 East Asia: CUACE/Dust, Atmos. Chem. Phys. Discuss., 7, 7987–8015, 2007,  
<http://www.atmos-chem-phys-discuss.net/7/7987/2007/>.

ACPD

7, 9115–9138, 2007

---

**SDS observation in  
East Asia**

Y. Q. Wang et al.

---

Title Page

Abstract

Introduction

Conclusions

References

Tables

Figures

◀

▶

◀

▶

Back

Close

Full Screen / Esc

Printer-friendly Version

Interactive Discussion

EGU

SDS observation in  
East Asia

Y. Q. Wang et al.

**Table 1.** The descriptions of SDS station network in China.

Station	Latitude (° N)	Longitude (° E)	Altitude (m)	Location	Measurement
Tazhong	39.00	83.67	1099.3	Center of the Taklimankan Desert	PM <sub>10</sub> , visibility
Hetian	37.13	79.93	1374.6	Southern margin of the Taklimakan Desert	PM <sub>10</sub>
Hami	42.82	93.52	737.2	Eastern Xinjiang province	PM <sub>10</sub> , visibility
Ejinaqi	41.95	101.07	940.5	Northern margin of the Badain Juran Desert	PM <sub>10</sub> , visibility
Dunhuang	40.15	94.68	1139.0	Eastern margin of the Kumtag Desert	PM <sub>10</sub> , visibility
Jiuquan	39.77	98.48	1477.2	Western margin of the Badain Juran Desert	PM <sub>10</sub> , visibility
Minqin	38.63	103.08	1367.0	Western margin of the Tengger Desert	PM <sub>10</sub> , visibility
Zhurihe	42.40	112.90	1150.8	Southeastern Onqin Dage sandy land	PM <sub>10</sub>
Wulatezhongqi	41.57	108.52	1288.0	Steppe area in mid-inner Mongolia	PM <sub>10</sub> , visibility
Zhangbei	41.15	114.70	1393.3	Downwind area of east China	PM <sub>10</sub> , visibility
Datong	40.10	113.33	1067.2	Notheastern margin of the Loess Plateau	PM <sub>10</sub>
Dongsheng	39.83	109.98	1460.4	Notheastern margin of the Mu Us Desert	PM <sub>10</sub>
Yushe	37.07	112.98	1041.4	Eastern Loess Plateau	PM <sub>10</sub> , visibility
Yan'an	36.60	109.50	958.5	Center of the Loess Plateau	PM <sub>10</sub>
Xilinhaote	43.95	116.07	989.5	North of Onqin Dage sandy land	PM <sub>10</sub> , visibility
Tongliao	43.60	122.37	178.5	East of Horqin sandy land	PM <sub>10</sub>
Beijing	39.80	116.47	31.3	Downwind area of east China	PM <sub>10</sub>
Dalian	38.90	121.63	91.5	Downwind area of east China	PM <sub>10</sub>
Huimin	37.48	117.53	11.7	Downwind area of east China	PM <sub>10</sub>

Title Page

Abstract

Introduction

Conclusions

References

Tables

Figures

◀

▶

◀

▶

Back

Close

Full Screen / Esc

Printer-friendly Version

Interactive Discussion

SDS observation in  
East Asia

Y. Q. Wang et al.

**Table 2.** Observed mean PM<sub>10</sub> concentration, visibility based on the data during SDS events and the PM<sub>10</sub> concentration values on visibility of 500 m, 1000 m and 10 000 m calculated from the fitting formula.

Data set	Number of data pairs	Mean PM <sub>10</sub> (μg m <sup>-3</sup> )	Mean Visibility (m)	Fitting formula	R <sup>2</sup>	PM <sub>10</sub> (μg m <sup>-3</sup> )		
						Visibility (500 m)	Visibility (1000 m)	Visibility (10 000 m)
Tazhong	349	2493.1	5926.2	$y=8E+07x^{-1.3466}$	0.8371	18 563	7299	329
Ejinaqi	40	514.2	16767.8	$y=8E+08x^{-1.6336}$	0.8953	31 193	10 053	234
Dunhuang	103	971.9	7331.5	$y=5E+07x^{-1.3088}$	0.7593	14 674	5923	291
Jiuquan	26	1149.6	12907.1	$y=6E+07x^{-1.3486}$	0.9085	13 751	5399	242
Minqin	21	657.0	11637.7	$y=6E+08x^{-1.6097}$	0.9108	27 141	8893	218
Zhurihe	37	1587.9	12404.9	$y=1E+08x^{-1.3687}$	0.9138	20 226	7832	335
Wulatezhongqi	19	753.8	9593.2	$y=3E+08x^{-1.4519}$	0.8956	36 182	13 226	467
Zhangbei	23	348.7	16439.5	$y=8E+06x^{-1.1303}$	0.6736	7 119	3252	241
Xilinhaote	38	652.2	14907.2	$y=1E+07x^{-1.1973}$	0.6951	5868	2559	162
All above Stations	656	1332.5	7153.5	$y=1E+08x^{-1.418}$	0.8506	14 889	5572	213

Title Page

Abstract

Introduction

Conclusions

References

Tables

Figures

◀

▶

◀

▶

Back

Close

Full Screen / Esc

Printer-friendly Version

Interactive Discussion

EGU

## SDS observation in East Asia

Y. Q. Wang et al.

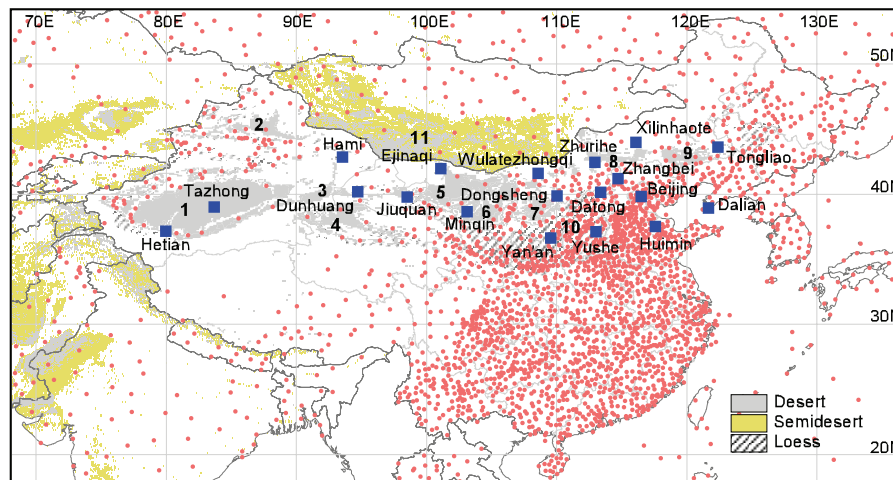


**Fig. 1.** The distribution map of the stations used to observation SDS in CMA. The red dots are weather stations while the blue squares are SDS observation stations. In this figure, the main SDS source regions are: 1, Taklimakan Desert; 2, Gurbantunggut Desert; 3, Kumtag Desert; 4, Qiadam Basin Desert; 5, Badain Juran Desert; 6, Tengger Desert; 7, Mu Us Desert; 8, Onqin Daga sandy land; 9, Horqin sandy land; 10, Loess Plateau; 11, Deserts and semideserts in Mongolia.

Title Page

Abstract

Introduction

Conclusions

References

Tables

Figures

◀

▶

◀

▶

Back

Close

Full Screen / Esc

Printer-friendly Version

Interactive Discussion

SDS observation in  
East Asia

Y. Q. Wang et al.

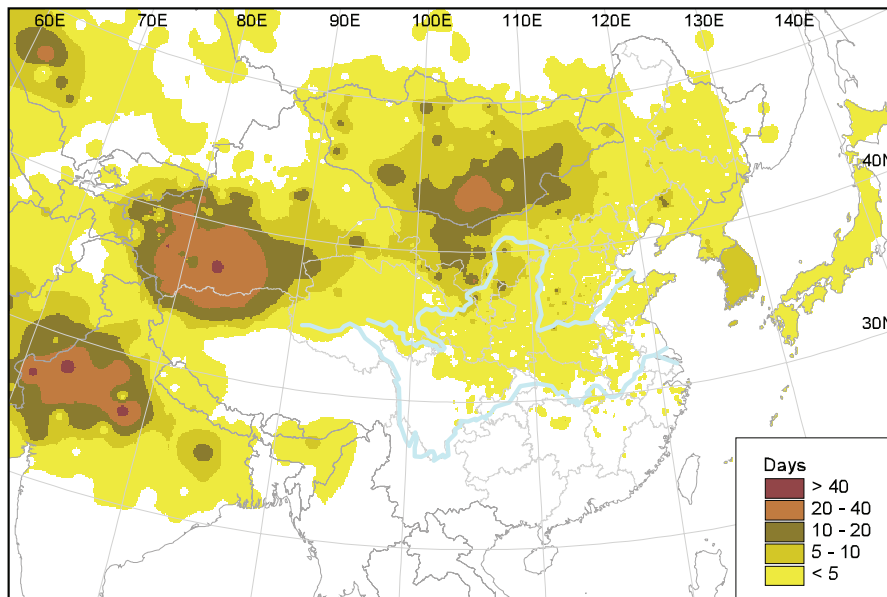


**Fig. 2.** The distribution of annual mean days of SDS events in spring from 2001 to 2006.

[Title Page](#)[Abstract](#)[Introduction](#)[Conclusions](#)[References](#)[Tables](#)[Figures](#)[◀](#)[▶](#)[◀](#)[▶](#)[Back](#)[Close](#)[Full Screen / Esc](#)[Printer-friendly Version](#)[Interactive Discussion](#)

EGU

SDS observation in  
East Asia

Y. Q. Wang et al.

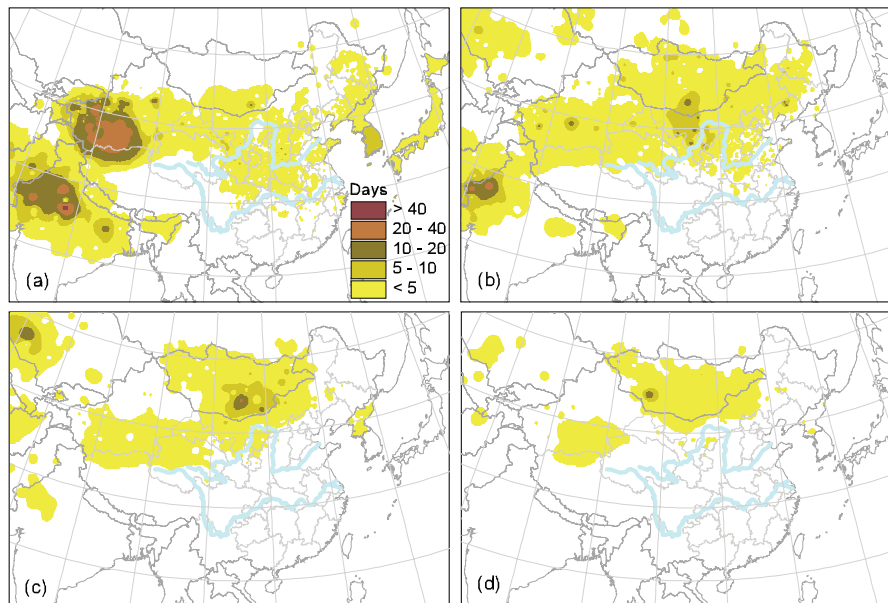


**Fig. 3.** The distribution of annual mean days of four categories of SDS events in spring from 2001 to 2006. **(a)** suspended dust; **(b)** blowing sand; **(c)** sand and dust storm; **(d)** severe sand and dust storm.

[Title Page](#)[Abstract](#)[Introduction](#)[Conclusions](#)[References](#)[Tables](#)[Figures](#)[I◀](#)[▶I](#)[◀](#)[▶](#)[Back](#)[Close](#)[Full Screen / Esc](#)[Printer-friendly Version](#)[Interactive Discussion](#)

EGU

SDS observation in  
East Asia

Y. Q. Wang et al.

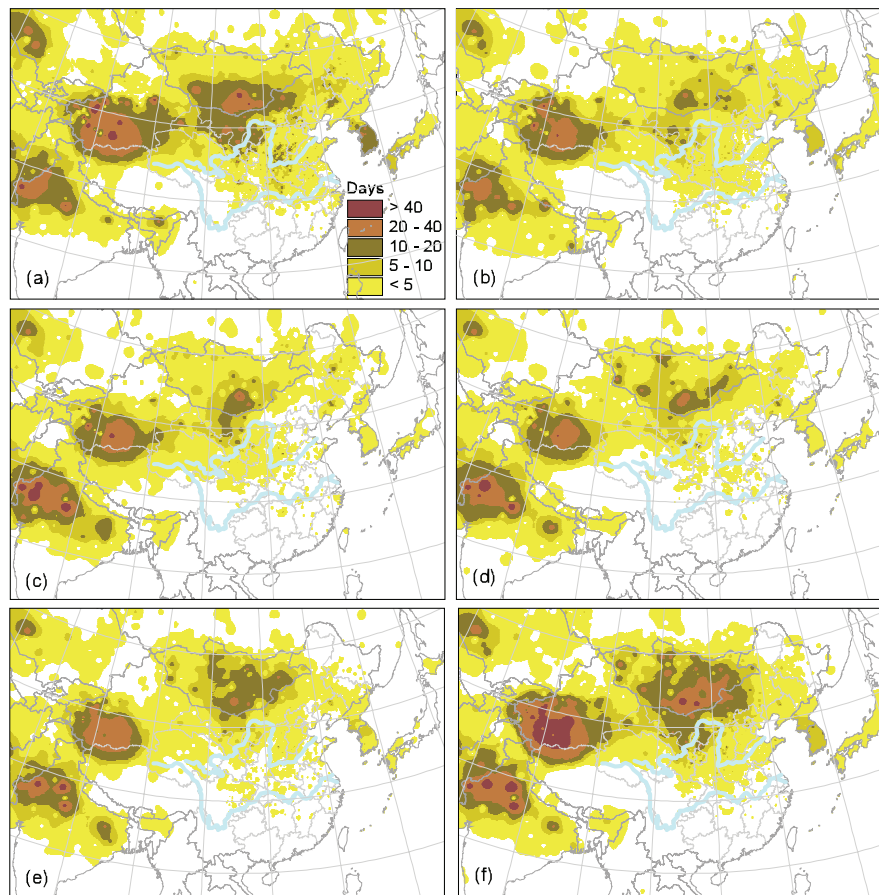


**Fig. 4.** The distribution of annual mean days of SDS events in spring from 2001 to 2006. **(a)** 2001; **(b)** 2002; **(c)** 2003; **(d)** 2004; **(e)** 2005; **(f)** 2006.

[Title Page](#)[Abstract](#)[Introduction](#)[Conclusions](#)[References](#)[Tables](#)[Figures](#)[I◀](#)[▶I](#)[◀](#)[▶](#)[Back](#)[Close](#)[Full Screen / Esc](#)[Printer-friendly Version](#)[Interactive Discussion](#)

## SDS observation in East Asia

Y. Q. Wang et al.

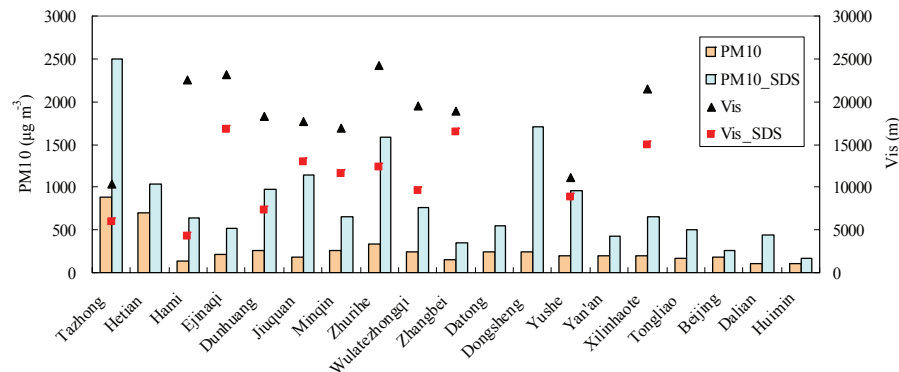


**Fig. 5.** The daily-averaged mean values of PM<sub>10</sub> concentration and visibility of each SDS observation station during the entire period and SDS events period of spring from 2004 to 2006. In the figure, the PM<sub>10</sub> mean concentrations for entire period and SDS events period are represented by orange and baby blue bars respectively, while the two kinds of visibility mean values are represented by black triangles and red squares.

Title Page

Abstract

Introduction

Conclusions

References

Tables

Figures

◀

▶

◀

▶

Back

Close

Full Screen / Esc

Printer-friendly Version

Interactive Discussion

EGU

## SDS observation in East Asia

Y. Q. Wang et al.

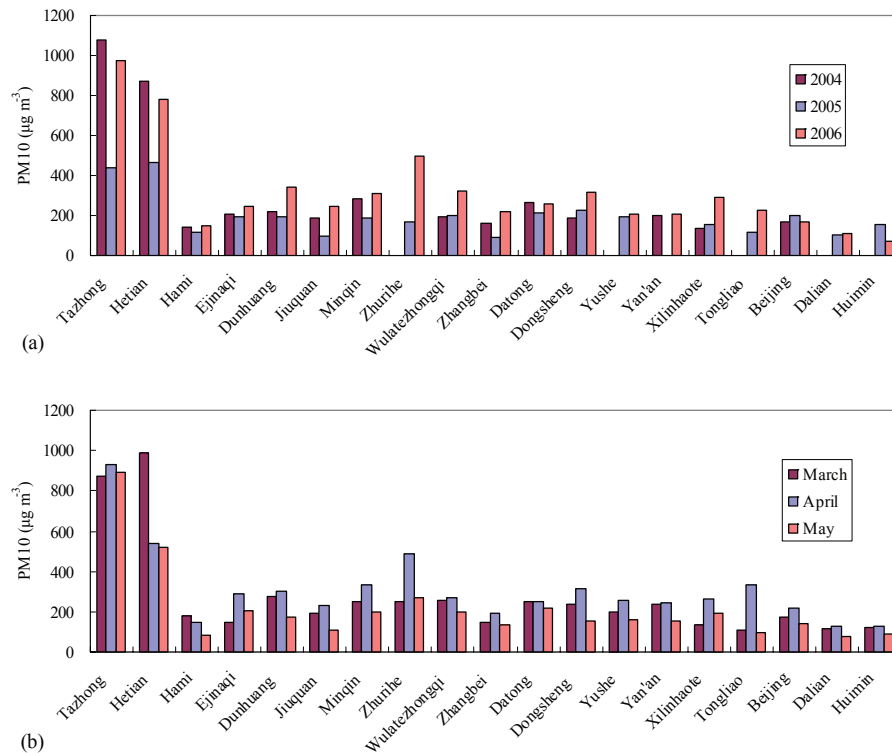


**Fig. 6. (a)** Annual and **(b)** monthly mean PM<sub>10</sub> mean concentration for each SDS observation station.

Title Page

Abstract

Introduction

Conclusions

References

Tables

Figures

◀

▶

◀

▶

Back

Close

Full Screen / Esc

Printer-friendly Version

Interactive Discussion

EGU

SDS observation in  
East Asia

Y. Q. Wang et al.

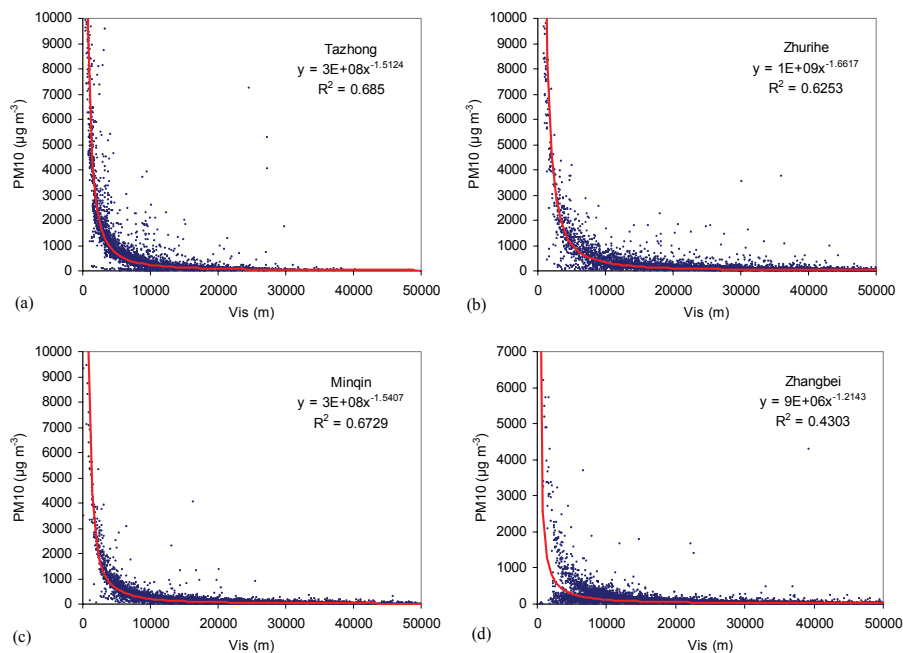


**Fig. 7.** Plot of hourly-averaged  $PM_{10}$  concentration vs. visibility during 3 spring seasons in the stations of (a) Tazhong, (b) Zhurihe, (c) Minqin and (d) Zhangbei.

[Title Page](#)[Abstract](#)[Introduction](#)[Conclusions](#)[References](#)[Tables](#)[Figures](#)[I◀](#)[▶I](#)[◀](#)[▶](#)[Back](#)[Close](#)[Full Screen / Esc](#)[Printer-friendly Version](#)[Interactive Discussion](#)

EGU

SDS observation in  
East Asia

Y. Q. Wang et al.

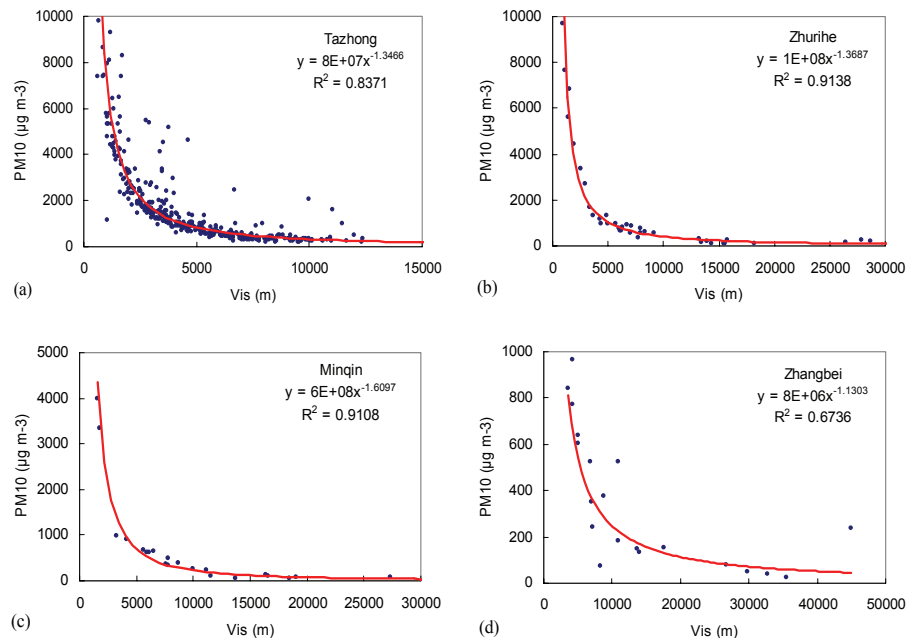


**Fig. 8.** Plot of hourly-averaged  $PM_{10}$  concentration vs. visibility during SDS events in the spring-time in the stations of **(a)** Tazhong, **(b)** Zhurihe, **(c)** Minqin and **(d)** Zhangbei.

[Title Page](#)[Abstract](#)[Introduction](#)[Conclusions](#)[References](#)[Tables](#)[Figures](#)[◀](#)[▶](#)[◀](#)[▶](#)[Back](#)[Close](#)[Full Screen / Esc](#)[Printer-friendly Version](#)[Interactive Discussion](#)

EGU